Spectral Methods in Causal Dynamical Triangulations

Giuseppe Clemente
giuseppe.clemente@pi.infn.it

Talk based on the paper 1804.02294, written in collaboration with Massimo D'Elia (massimo.delia@unipi.it)

Istituto Nazionale di Fisica Nucleare

IN SUPREMÆ DIGNITATIS 1343
Università di Pisa

"Numerical approaches to holography, quantum gravity and cosmology" workshop
Edinburgh, 22 May 2018

Overview

introduction

CDT overview
- formalism
- phase diagram and standard results

spectral methods
- physical motivation
- Weyl's law and effective dimension

numerical results
- spectral gap and spectral density
- Scaling and effective dimension for slices
- full spectral density

conclusions

The QG problem

Manifest difficulties:

- Standard perturbation theory fails divergences arise at short scale
- Gravitational quantum effects unreachable on lab: $E_{Pl} = \sqrt{\frac{\hbar c}{G}} c^2 \simeq 10^{19} GeV$ (big bang or black holes)

Two lines of direction in QG approaches

- non-conservative: introduce new short-scale physics
- conservative: do not give up on the Einstein theory

Causal Dynamical Triangulations (CDT): conservative approach of non-perturbative renormalization of the Einstein gravity via Monte-Carlo simulations.

CDT overview

Lattice regularization

A *regularization* makes the renormalization procedure well posed.

- discretize spacetime introducing a minimal **lattice spacing** 'a'
- localize dynamical variables on lattice sites
- study how quantities diverge for $a \to 0$
- Cartesian grids approximate Minkowski space
- **Regge triangulations** approximate generic manifolds

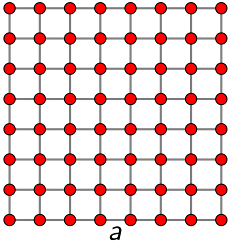

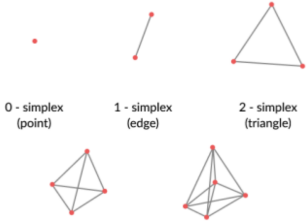

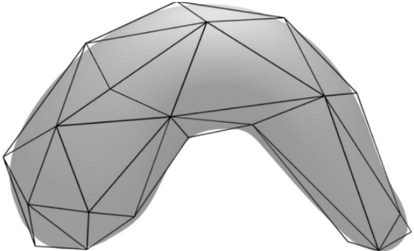

Causality condition

A Lorentzian (causal) structure on $\mathcal{T}$ can be enforced by using a *foliation* of spatial **slices** of constant proper time

- Vertices "live" in slices.
- d-simplexes fill spacetime between slices.
- Links can be spacelike with $\Delta s^2 = a^2$, or timelike with $\Delta s^2 = -\alpha a^2$.
- Only a finite number of simplex types.
- The α parameter is used later to perform a Wick-rotation from Lorentzian to Euclidean

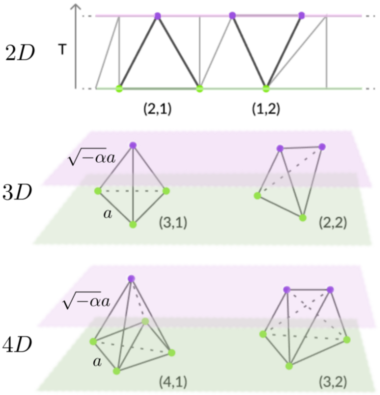

Regge formalism: action discretization

Also the EH action must be discretized accordingly ($g_{\mu\nu} \to \mathcal{T}$):

$$S_{EH}[g_{\mu\nu}] = \frac{1}{16\pi G}\left[\underbrace{\int d^d x \sqrt{|g|}\, R}_{\text{Total curvature}} - 2\Lambda \underbrace{\int d^d x \sqrt{|g|}}_{\text{Total volume}}\right]$$

$\Downarrow$ discretization $\Downarrow$

$$S_{Regge}[\mathcal{T}] = \frac{1}{16\pi G}\left[\sum_{\sigma^{(d-2)}\in\mathcal{T}} 2\varepsilon_{\sigma^{(d-2)}} V_{\sigma^{(d-2)}} - 2\Lambda \sum_{\sigma^{(d)}\in\mathcal{T}} V_{\sigma^{(d)}}\right],$$

where $V_{\sigma^{(k)}}$ is the k-volume of the simplex $\sigma^{(k)}$.

Wick-rotation $iS_{Lor}(\alpha) \to -S_{Euc}(-\alpha)$

$\implies$ Monte-Carlo sampling $\mathcal{P}[\mathcal{T}] \equiv \frac{1}{Z}\exp(-S_{Euc}[\mathcal{T}])$

Wick rotated action in 4D

At the end of the day [Ambjörn et al., arXiv:1203.3591]:

$$S_{CDT} = -k_0 N_0 + k_4 N_4 + \Delta(N_4 + N_4^{(4,1)} - 6N_0)$$

- New parameters: (k_0, k_4, Δ), related respectively to G, Λ and α.
- New variables: N_0, N_4 and $N_4^{(4,1)}$, counting the total numbers of vertices, pentachorons and type-$(4,1)/(1,4)$ pentachorons respectively ($\mathcal{T}$ dependence omitted).

It is convenient to "fix" the total spacetime volume $N_4 = V$ by fine-tuning $k_4 \implies$ actually free parameters (k_0, Δ, V).

Simulations at different volumes V allow finite-size scaling analysis.

Monte-Carlo: sum over causal geometries

Configuration space in CDT: triangulations with **causal structure**

Lorentzian (causal) structure on $\mathcal{T}$ enforced by means of a *foliation* of spatial **slices** of constant proper time.

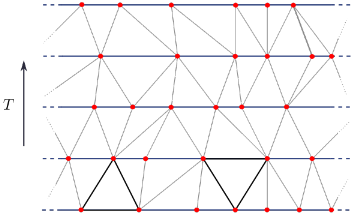

Path-integral over causal geometries/triangulations $\mathcal{T}$ using Monte-Carlo sampling by performing local updates. E.g., in 2D:

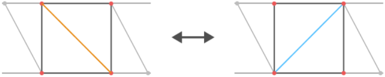

flipping timelike link

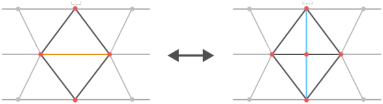

creating/removing vertex

Ultimate goal

Find a second order critical point in the phase diagram
$\Longrightarrow$ **renormalize the theory**.

Continuum limit

The system must forget the lattice discreteness: second-order critical point with divergent correlation length $\hat{\xi} \equiv \xi/a \to \infty$

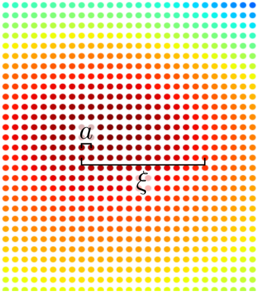

Asymptotic freedom (e.g. QCD):

$$\vec{g}_c \equiv \lim_{a\to 0} \vec{g}(a) = \vec{0}$$

Asymptotic safety (maybe QG):

$$\vec{g}_c \equiv \lim_{a\to 0} \vec{g}(a) \neq \vec{0}$$

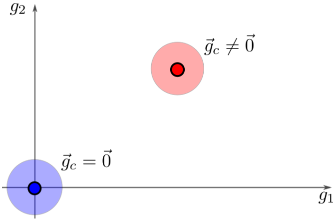

Phase diagram of CDT in 4D

k_4 "tuned" to fix $V \implies$ remaining free parameters: (k_0, Δ)

phase	spatial volume per slice
A:	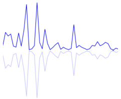
B:	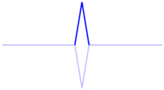
C_{dS}/C_b:	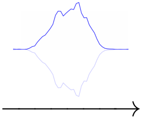

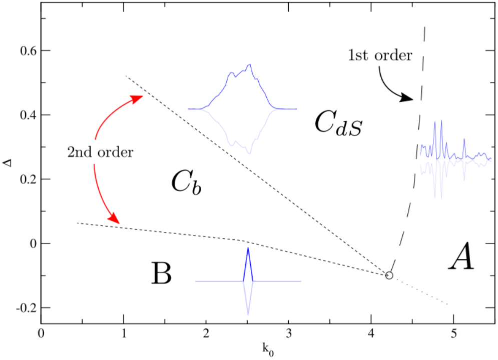

possible 2nd order lines have been found [1108.3932,1704.04373]
C_b and C_{dS} differ by the geometry of slices (discussed later)

C_{dS}: "de Sitter" phase

- Time-extended distribution of the triangulation/Universe (blob)
- Average of blob profiles over configurations has the same distribution of the **de Sitter cosmological model**: the best description of the physical Universe dominated by dark energy!
- Fluctuations of spatial volume interpreted as quantum effects

Lorentzian: $$-x_0^2 + x_1^2 + x_2^2 + x_3^2 + x_4^2 = R^2$$

$\Downarrow$ analytic continuation $\Downarrow$

Euclidean: $$+x_0^2 + x_1^2 + x_2^2 + x_3^2 + x_4^2 = R^2$$

De Sitter spatial volume distribution

$$V_s^{(dS)}(t) = \frac{V_{tot}}{2}\frac{3}{4}\frac{1}{\widetilde{s}(V_{tot})^{\frac{1}{4}}}\cos^3\left(\frac{t}{\widetilde{s}(V_{tot})^{\frac{1}{4}}}\right)$$

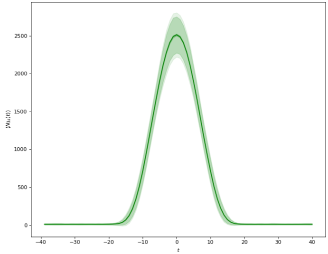

Problem: lack of observables

A proper investigation of the continuum limit should require a possibly complete set of geometric observables.

Observables currently employed in CDT

- Spatial volume per slice: $V_s(t)$
  (number of spatial tetrahedra at the slice labeled by t)
- Order parameters for transitions:
  - $\text{conj}(k_0) = N_0/N_4$ for the $A|C_{dS}$ transition
  - $\text{conj}(\Delta) = (N_4^{(4,1)} - 6N_0)/N_4$ for the $B|C_b$ transition
  - OP_2 for the $C_b|C_{dS}$ transition
    [Ambjorn et al. arXiv:1704.04373]
- Fractal dimensions: (actually give some info at different scales)
  - spectral dimension
  - Hausdorff dimension

No observable characterizing geometries at all lattice scales!!

spectral methods

Proposed solution: spectral analysis

Spectral analysis

analysis of eigenvalues and eigenvector of the **Laplace-Beltrami operator**: $-\nabla^2$

Familiar examples:

- Fourier analysis in $[0, T]$ or $\mathbb{R}^N$:
  eigenvalues: $\lambda_k = k^2$
  eigenvectors: sines and cosines
- On the unit sphere S^2:
  eigenvalues: $\lambda_l = l(l+1)$
  degeneracy: $\mu_l = 2l+1$
  eigenvectors: spherical harmonics $Y_{l,m}$

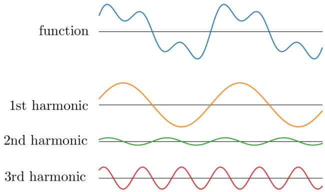

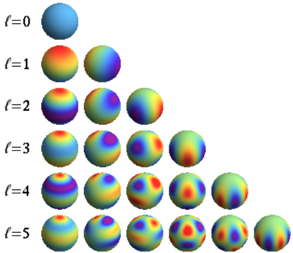

Hearing the shape of a manifold

- Spectral analysis on smooth manifolds $(\mathcal{M}, g_{\mu\nu})$:

$$-\nabla^2 f \equiv -\frac{1}{\sqrt{|g|}}\partial_\mu(\sqrt{|g|}g^{\mu\nu}\partial_\nu f) = \lambda f, \text{ with boundary conditions}$$

Can one hear the shape of a drum?

Almost: beside spectra you need also eigenvectors.

Example:
disk drum

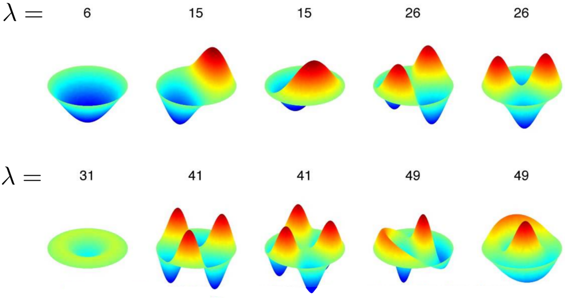

Spectral graph analysis

Graph: tuple $G = (V, E)$ where

V set of **vertices** v

E set of **edges**, unordered pairs of adjacent vertices $e = (v_1, v_2)$

Laplace matrix acting on functions of vertices $\vec{f} = (f(v)) \in \mathbb{R}^{|V|}$:

$$L = D - A$$

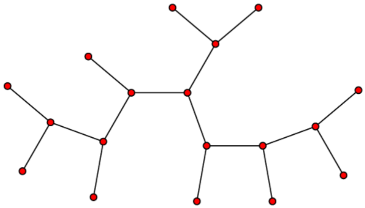

- $D_{v,v} =$"order of the vertex v (number of departing edges)"
- $A_{v_1,v_2} = 1$ if $(v_1, v_2) \in E$, zero otherwise

Spectral graph analysis of CDT slices

Observation

Spatial slices in CDT are made by identical $(d-1)$-simplexes
$\Longrightarrow$ a d-regular undirected graph is associated to any spatial slice.

- Spatial tetrahedra become vertices of associated graph
- Adjacency relations between tetrahedra become edges
- Laplace matrix: $L = D - A$, where $D = d\mathbb{1}$ is the *degree matrix* and A is the *adjacency matrix*.
- Eigenvalue problem $L\vec{f} = \lambda\vec{f}$ solved by numerical routines

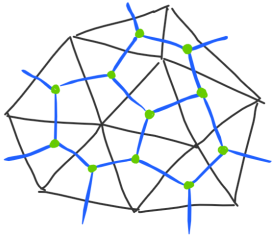

2D slice and its dual graph

Physical interpretation of LB eigenvalues and eigenvectors

Heat/diffusion equation on a manifold (or graph) M:

$$\partial_t u(x;t) - \Delta u(x;t) = 0\,.$$

General solution in a basis $\{e_n\}$ of LB eigenvectors ($\lambda_n \leq \lambda_{n+1}$):

$$u(x;t) = \sum_{n=0}^{|\sigma_M|-1} e^{-\lambda_n t}\widetilde{u}_n(0)e_n(x)\,.$$

consequences:

- λ_n is the diffusion rate for the (eigen)mode $e_n(x)$
- smallest eigenvalues $\leftrightarrow$ slowest diffusion directions.
- a large **spectral gap** λ_1 implies a fast overall diffusion, geometrically meaning a highly connected graph.

Interpretation of the spectral gap

spectral gap and eigenvector (Fiedler vector)

First (non-zero) eigenvalue λ_1 and its associated eigenvector e_1. The **spectral gap**, λ_1 measures the connectivity of the graph: the larger, the more connections between vertices.

Applications of the Fiedler vector e_1:

- Min-cut: minimal set of edges disconnecting the graph if cut
- Fiedler ordering on regular graphs (like CDT slices): core of the Google Search engine, and paramount reason for the Google's rise to success.
- many others...

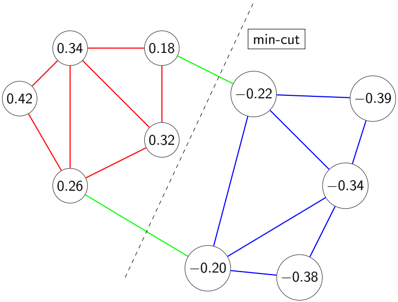

Weyl's law and effective dimension

For a manifold M with LB spectrum σ_M define:
$n(\lambda) \equiv \sum_{\bar{\lambda} \in \sigma_M} \theta(\bar{\lambda} - \lambda) =$ "number of eigenvalues below λ".

Weyl's law

Well known asymptotic result from spectral geometry:

$$n(\lambda) \sim \frac{\omega_d}{(2\pi)^d} V \lambda^{d/2},$$

being ω_d the volume of a unit d-ball and V the manifold volume.

Motivated by Weyl's law we define the **effective dimension**:

$$d_{EFF}(\lambda) \equiv 2 \frac{d \log(n/V)}{d \log \lambda}.$$

A toy model: toroidal lattice

Consider a 3-d periodic lattice with sizes $L_x \times L_y \times L_z$.

eigenvalues:

$$\lambda'_{\vec{m}} = 4\pi^2 \left(\frac{m_x^2}{L_x^2} + \frac{m_y^2}{L_y^2} + \frac{m_z^2}{L_z^2} \right) ,$$

with $m_i \in (-L_i/2, L_i/2\,] \cap \mathbb{Z}$.

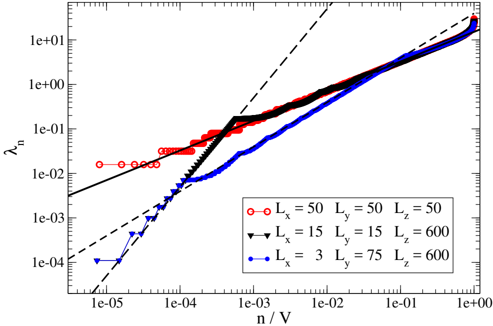

- Three regimes observed for $L_x \ll L_y \ll L_z$ with $d_{EFF} = 1, 2, 3$.
- Position of knees related to the scale of dimensional transition.

numerical results

Numerical simulations of 4D CDT

Simulations performed for total spatial volumes $N_{3s} = 20k, 40k$

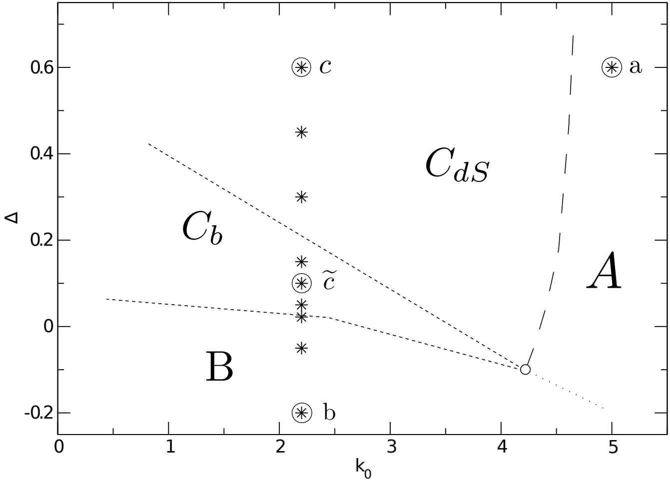

Spectral gap in different phases

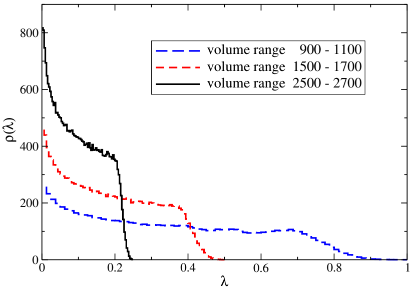

C_{dS} phase (first 100 eigenvalues)

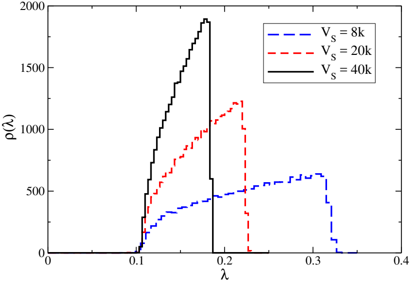

B phase (first 100 eigenvalues)

- no spectral gap in C_{dS} phase.
- non-zero spectral gap for slices in B phase (high connectivity).
- some volume dependence is present (except for λ_1 in B phase)

Collapse of scaling curves

The volume dependence can be reabsorbed by mapping λ_n vs n/V
$\Longrightarrow$ curves collapse into a volume independent function.

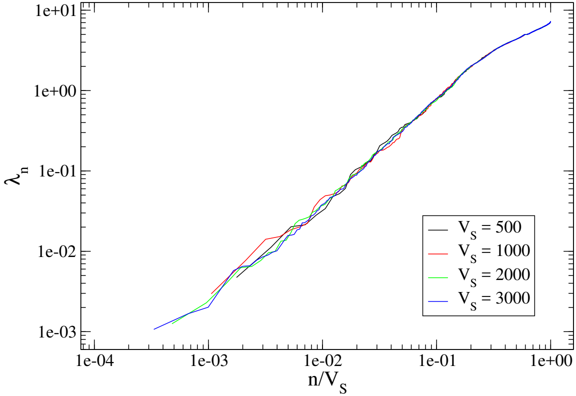

Weyl scalings for few slice in C_{dS} phase and different volumes

Scalings for different phases

By averaging over many slices (C_b discussed later):

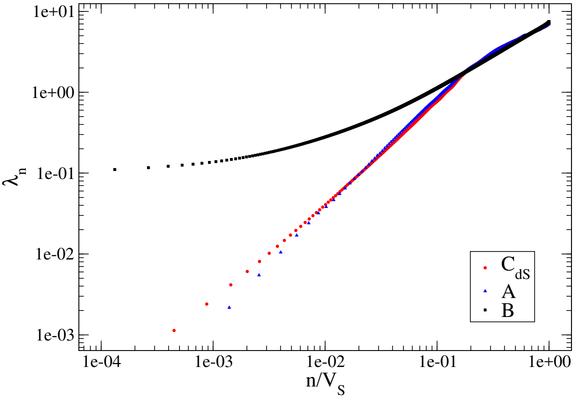

small λ (large scale) behaviour:

- vanishing spectral gap and finite slope for C_{dS} and A phases
- non-zero spectral gap and vanishing slope for B phase

Effective dimension for different phases

From the previous curves and the definition of **effective dimension**: $d_{EFF} \equiv 2\frac{d\log(n/V)}{d\log\lambda}$.

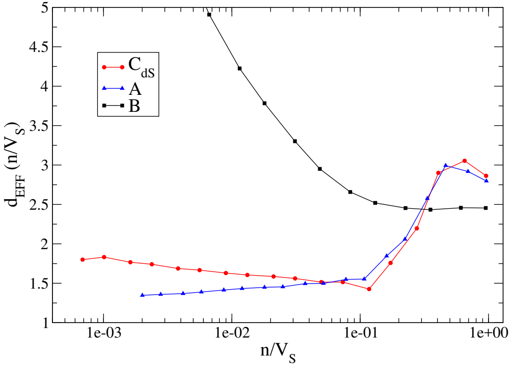

- $d_{EFF} \to \infty$ at large scales for B phase
- $d_{EFF} < 3$ for C_{dS} (and A) phase! $\implies$ fractional dimension

The bifurcation phase C_b

Similarities with C_{dS}:

- configurations with time extended blob (but narrower w.r.t. C_{dS} ones with the same k_0)
- similar spatial volume per slice $V_s(t)$

Main distinguishing feature (as known from previous literature):

- two classes of spatial slices, alternated in slice time, one of which possesses vertices with very high coordination number.

$\Longrightarrow$ Order parameter of C_b-C_{dS} transition defined in literature as relative difference between maximal coordination numbers of vertices in adjacent slices.

Alternating spectra in C_b configurations

Comparisons between C_{dS} and C_b low lying spectra:

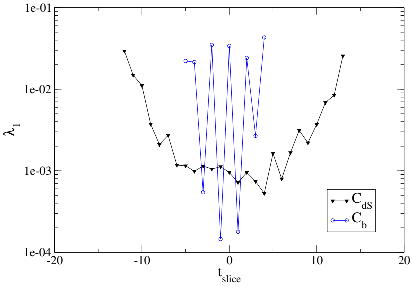

spectral gap for single configurations

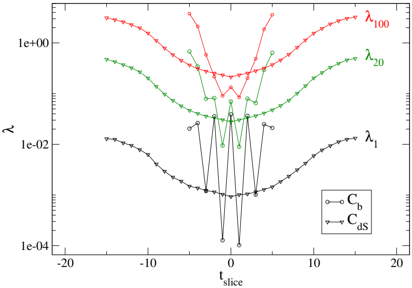

selected eigenvalues averaged over many configurations

The low lying spectra capture well the alternating behaviour of slice geometries in C_b configurations, and show it is a difference in large scale properties of slices.

Bifurcated scaling and class separation in C_b phase

Not a single scaling curve for C_b configurations
$\Longrightarrow$ a separation into two classes of slices is required:

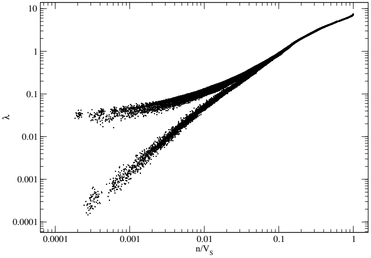

scatter plot λ vs n/V

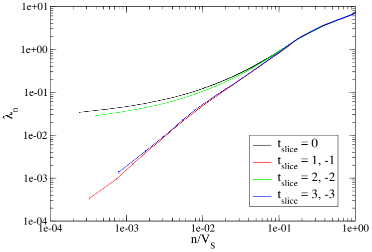

averaged values for different classes

We called the classes B-type and dS-type (for obvious reasons).

Spectral gap through phases

Spectral gap histogram for simulations with $k_0 = 2.2$ and different Δ:

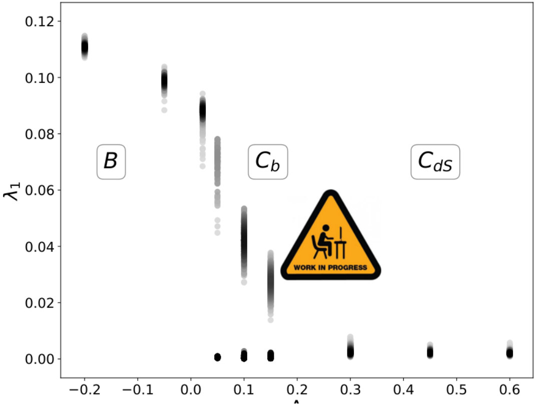

We are currently investigating the continuum limit around C_{dS}-C_b.

Full spectral density: B phase

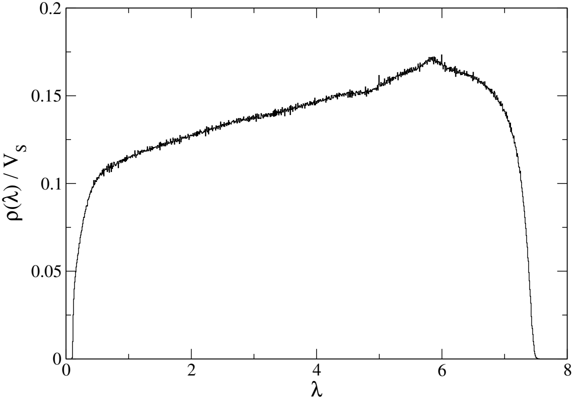

- nothing particularly interesting: almost uniform above the spectral gap
- shares similar features to random regular graphs ($d_{EFF} \to \infty$), but actually differ in spectrum.

Full spectral density: C_{dS} phase

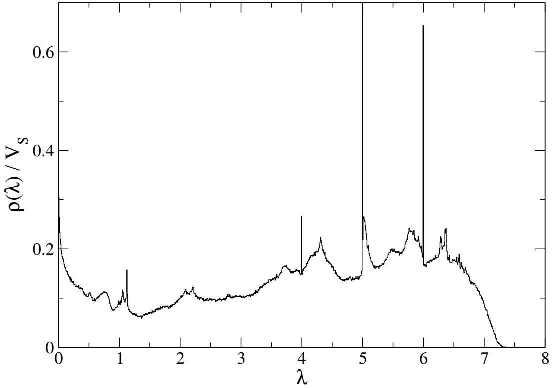

- Peaks at integer values $\lambda = 4, 5, 6$ have high multiplicity and correspond to extremely localized eigenvectors. (UV artefacts $\implies$ uninteresting)
- no theory on how to interpret peaks in the background...

conclusions

Summary

- CDT as a nonperturbative approach to renormalize gravity via Monte Carlo simulations
- promising results: seemingly 2nd order lines, “de Sitter” phase
- problem: continuum limit and lack of observables
- proposed spectral methods in order to obtain a hierarchy of geometric observables
- analysis of spectra of spatial slices:
  - spectral gap characterizes connectivity in different phases
  - Weyl’s scaling allow to define a running effective dimensionality
  - full spectral densities show non-trivial and interesting features

Further work

- generalize to full spacetime configurations (FEM methods required)
- apply to EDT configurations ("straightforward")
- analyze all the features of eigenvectors (possessing the remaining information about the geometry), i.e. Anderson localization, Morse analysis, etc...
- investigate continuum limit (currently work in progress)

Backup slides

Renyi entropy as a measure of localization

Renyi entropy : $S_\alpha(k) = \frac{1}{1-\alpha} \log \left(\sum_x (e_k(x))^{2\alpha} \right)$.

- $\alpha \to 1$: Shannon entropy
- $\alpha = 2$: Inverse Partecipation Ratio (IPR)

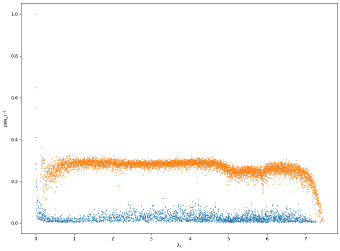

PR for C_{dS} and B slice eigenvectors

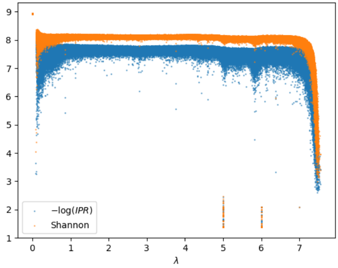

IPR and Shannon entropy for B slice eigenvectors

Laplacian embedding

Laplacian embedding: embedding of graph in k-dimensional (Euclidean) space, solution to the optimization problem:

$$\min_{\vec{f}^1,\dots,\vec{f}^k} \Big\{ \sum_{(v,w)\in E} \sum_{s=1}^{k} [f^s(v) - f^s(w)]^2 \mid \vec{f^s} \cdot \vec{f^p} = \delta_{s,p},\ \vec{f^s} \cdot \vec{1} = 0 \ \forall s, p = 1, \dots, k \Big\},$$

where for each vertex $v \in V$ the value $f^s(v)$ is its s-th coordinate in the embedding.

The solution $\{f^s(v)\}_{s=1}^{k}$ is exactly the (orthonormal) set of the first k eigenvectors of the Laplace matrix $\{e_s(v)\}_{s=1}^{k}$!

Laplacian embedding: example torus $T^2 = S^1 \times S^1$

For each graph-vertex $v \in V$ plot the tuple of coordinates:

2D: $(e_1(v), e_2(v)) \in \mathbb{R}^2$

3D: $(e_1(v), e_2(v), e_3(v)) \in \mathbb{R}^3$

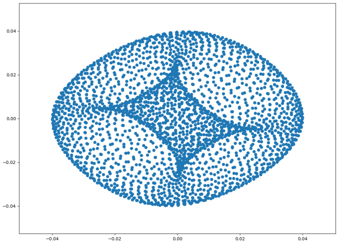

(a) 2D embedding

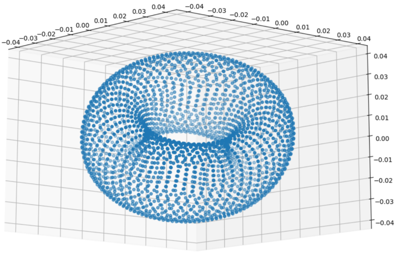

(b) 3D projected embedding

Laplacian embedding of spatial slices in C_{dS} phase

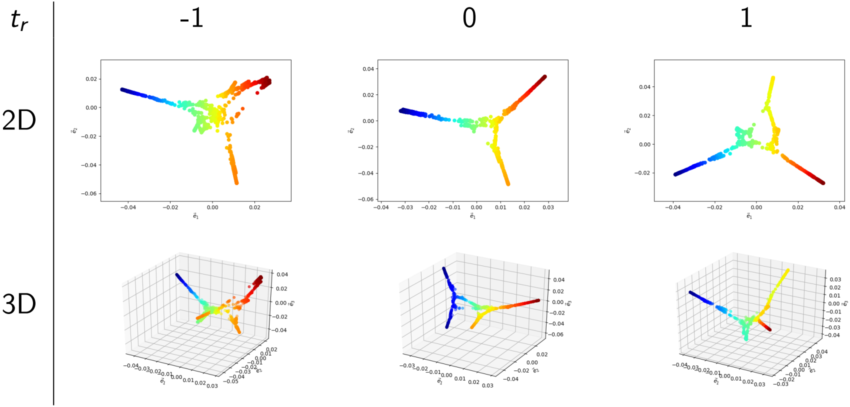

The first three eigenstates are not enough to probe the geometry of substructures

3D Laplacian embedding of T^3 torus

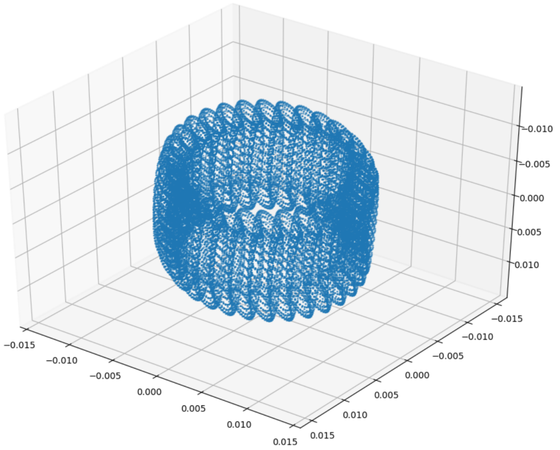

$$T^3 \cong T^2 \times S^1 \cong S^1 \times S^1 \times S^1$$

Result: spectral clustering of C_{dS} spatial slices

Spectral clustering: recursive application of min-cut procedure

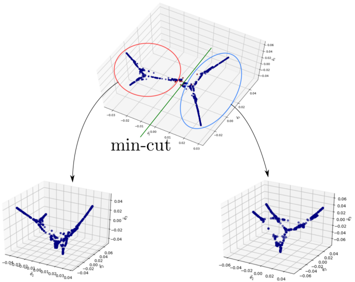

Qualitative picture (2D)

Observation: fractality

Self-similar filamentous structures in C_{dS} phase (S^3 topology)

Spectral dimension D_S

Computed from the return probability for random-walks on manifold or graph: $P_r(\tau) \propto \tau^{-\frac{D_S}{2}} \implies D_S(\tau) \equiv -2\frac{d \log P_r(\tau)}{d \log \tau}$.

- Usual integer value on regular spaces: e.g. $D_S(\tau) = d$ on $\mathbb{R}^d$
- τ-independent fractional value on true fractals
- τ-dependent fractional value in general (some scale involved)

Equivalent definition of return probability: $P_r = \frac{1}{|V|}\sum_k e^{-\lambda_n t}$

$\implies$ Nice interpretation of return probability in terms of diffusion processes (random-walks): smaller eigenvalues $\leftrightarrow$ slower modes. The smallest non-zero eigenvalue λ_1 represents the **algebraic connectivity** of the graph.

The spectral dimension on C_{dS} slices

Compare P_r obtained by explicit diffusion processes or by the LB eigenspectrum

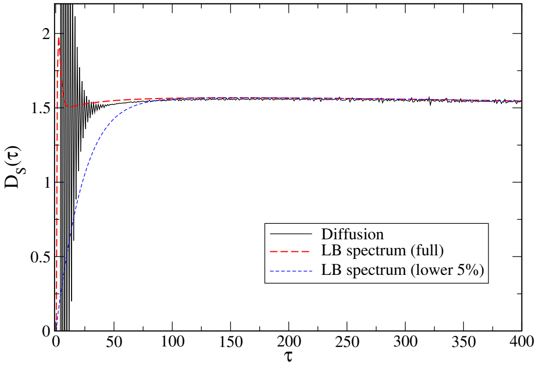

fractional value $D_S(\tau) \simeq 1.5 \implies$ fractal distribution of space.